18th International Conference on Sheet Metal, SHEMET 2019

# Haptic metal spinning

Iacopo M. Russo[a], Christopher J. Cleaver[a], Julian M. Allwood[a,*]

*[a] Department of Engineering, University of Cambridge, Trumpington Street, Cambridge CB2 1PZ, UK*

## Abstract

Sheet metal spinning is an incremental forming technique practiced for a long time only by experienced, skilled craftsmen. Over the last sixty years, attempts have been made to automate the process, but today the industrial practice still relies heavily on the skill of experienced operators. Complete analytical solutions to predict workpiece failure based on the path of the tool are not available, and finite element simulations of the process are too time-intensive to be of practical use for online toolpath correction. Therefore, today the design of toolpaths to avoid failure in spinning remains an art acquired by practice. In this paper, we approach the issue by designing an enhanced teach-in/playback system. We connect a haptic device to a CNC spinning machine; this device allows a human operator to control the working roller manually while feeling the force applied to the workpiece. Position, force and workpiece shape sensors allow collecting information on the toolpath followed by the operator and on its influence over the mechanics of the process. The opportunities offered by this system to derive rules for toolpath design are explored in two case studies on force control and wrinkling recovery, with new insights on the relationship between toolpaths and failure. A research agenda is outlined to exploit the full potential of haptic metal spinning.

*Keywords:* metal spinning; toolpath design; force control; haptic interface; bilateral teleoperation

## 1. Introduction

Sheet metal spinning is a technique to incrementally form hollow axisymmetric components from circular blanks. For centuries, spinning has been performed manually by experienced craftsmen, who use stick-type tools to progressively form a flat blank into the shape set by a mandrel, making objects such as metal vases, pots and trophies [1]. With

---

\* Corresponding author. Tel.: +44 (0) 1223 748271
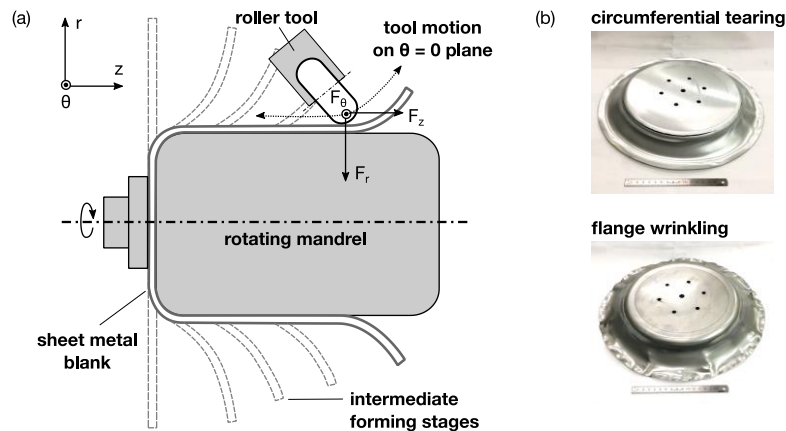*E-mail address:* jma42@cam.ac.uk

Fig. 1. (a) The conventional sheet metal spinning process, in which a roller tool moving on a plane progressively forms a blank onto a rotating mandrel; the tool forces are noted. (b) Photographs of workpieces showing the two main modes of failure in spinning: tearing and wrinkling.

practice, a craftsman can accumulate the experience required to spin a variety of shapes and materials without causing premature failure of the workpiece. This experience is based on multiple sensory channels (visual, auditory and tactile) and has proved hard to translate into the rules that would be needed to design an automatic version of the process.

Nonetheless, in the last sixty years progress has been made in designing metal spinning processes and machines for industrial production. As shown in Fig. 1(a), the craftsmen's stick has been replaced by a roller tool, which is made to follow a path either programmed by computer-numerical-control (CNC) or performed manually by a human operator and then recorded by a teach in/playback system. CNC is usually applied when components can be formed in a single toolpass, as in the case of shear spinning of cones. When more complex shapes are to be formed (with features such as straight or re-entrant walls), multiple forward and backward passes are needed, and the design of the toolpath is still left to an experienced operator whose actions are recorded and re-played for the subsequent runs.

In academia, experimental and numerical studies into toolpath design have attempted to find the best toolpath to avoid workpiece failure [2], which can occur either by tearing or wrinkling, Fig. 1(b). Based on experiments, Hayama et al. [3] suggested that concave involute toolpass geometries give the best results, and Liu et al. [4] supported their thesis through FE analysis. Instead, Wang and Long [5] found experimentally that convex toolpaths minimise both tool forces and thinning. Results from the literature are sometimes contradictory and anyway still insufficient for the design of a complete toolpath. Polyblank [6] tentatively demonstrated a finite horizon control system in which failure is checked only for a short time into the future using an accurate finite element (FE) model, but found the system too slow for industrial use: the design of a single toolpass would take weeks to complete.

Therefore, here we propose an enhanced teach in/playback system suitable for academic research, based on the use of a haptic device. The word 'haptic' derives from the Greek word *haptikos*, meaning 'pertaining to the sense of touch'. Haptic devices provide users with force feedback and have found applications in fields as diverse as robotic surgery and gaming [7]. In manufacturing, they have been employed mostly to interact with computer-generated environments in design and assembly of components [8], but in other fields they have been employed for bilateral teleoperation, i.e. to remotely operate machines interacting with real environments [9]. To the authors' knowledge, the application of devices providing force feedback to the user has not been reported in the metal forming literature.

In the next section, the developed haptic metal spinning set-up is presented. Then, the results of two case studies are reported to give a first demonstration of the opportunities offered by this system in the study of toolpath design and failure in conventional spinning.

## 2. Haptic metal spinning: the set-up

The overall purpose of haptic metal spinning is to allow a human operator to manually control the roller and to feel the force applied to the workpiece, all the while recording their actions with multiple sensors. This section presents the bilateral teleoperation system developed to achieve this. It lists the technical specifications of the haptic device (HDevice) used, it presents the system elements required to send motion commands to the roller tool and feed force

information back to the user, and it describes the ergonomic arrangement of the HDevice and the charts providing visual feedback from computer screens.

The teleoperation system is presented in Fig. 2. The Phantom Desktop haptic device is used [10], a stylus-based device originally manufactured and sold by SensAble, Inc. (today the device is called Touch X and is marketed by 3D Systems, Inc.). The device has 6 positional degrees of freedom (DoF) and can provide force feedback in 3 directions. The position of the stylus is sensed by optical encoders, while small electric DC motors provide the actuation for force feedback. The physical workspace in which force can be exerted is $160 \times 120 \times 120$ mm in local $(x, y, z)$ coordinates, while the maximum displayable force is 7.5 N. All other technical specifications can be found online [11]. The device is connected via parallel port connection to a computer running Windows 7. Haptic applications with the Phantom Desktop are programmed using OpenHaptics, a free-to-download, C-based application programming interface (API). The routines contained in the API allow low-level access to the device: the current position of the stylus can be read and forces can be commanded. To ensure stability, functions to get and set the device state are managed by a scheduler in a high-priority thread via asynchronous function callbacks.

The spinning machine built by Music and Allwood at the University of Cambridge [12] is employed. The working roller (WRoller) is actuated by two servomotors. It can move on a plane in the radial ($r$) and axial ($z$) direction, as illustrated in Fig. 1. Motion is controlled by a National Instruments (NI) real-time controller; motion applications are programmed using NI LabVIEW software. Information is transferred between the computer and the real-time controller using LabVIEW's shared variables, i.e. variables that can be published across an Ethernet-network. Motion applications are programmed using the LabVIEW SoftMotion module and the Contour-Move move type is used to implement manual operation of the roller. In this move type, commanded positions can be updated continuously in a buffer table; the controller generates the trajectory and ensures that the WRoller moves through the commanded positions. The time delay between the motion of the WRoller and the HDevice, as measured by video analysis, is $0.3 \pm 0.06$ s. Loadcells with a nominal range of 2.0 and 1.5 kN are installed on the radial and axial motion axis of the WRoller, respectively.

In the bilateral transfer of information, scaling factors are necessary for both the position and the force. Based on the dimension of the blank (see section 2.1) and the expected axial motion, WRoller/HDevice position scaling factors of 0.4-0.8 were used in the case studies below. Force is commanded to the HDevice using motor torque counts. The force in N applied to the operator's hand depends on the position of the stylus; at $(x, y, z = 0)$ it was found that WRoller/HDevice force scaling factors of 0.001-0.002 were enough for the operator to experience significant force feedback (1.5 to 3 N of force exerted on the operator's hand).

Finally, it is worth describing the arrangement of the desk where manual operation of the HDevice occurs. A photograph and computer screenshots are shown in Fig. 3. Because only two DoFs are required to fully control the WRoller, the under-constrained haptic device stylus is made to rest on an elevated platform to fix its position in the $z$-direction. The operator wields the stylus in a way not dissimilar to writing and can freely move on a plane while
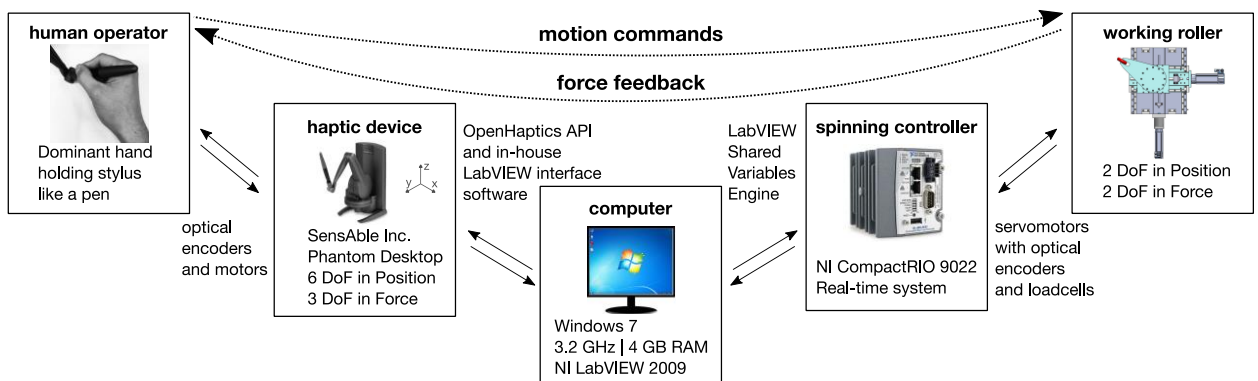


Fig. 2. The bilateral teleoperation system implemented using the haptic device. As the operator moves the stylus, position changes are sensed and motion commands are sent to the working roller; as the roller applies force to the workpiece, forces are sensed and fed back to the operator.

Fig. 3. The haptic spinning desk set-up. The operator holds the haptic device stylus like a pen over a wide flat support. On the computer screens, a webcam and several charts provide the operator with visual feedback on the progress of forming: positions, forces and workpiece shape.

resting the wrist on the platform, thus avoiding fatiguing the wrist joint during the process. The HDevice is orientated so that its *x*-direction aligns with the *z*-direction of the WRoller space, and its *y*-direction aligns with the *r*-direction. This is so that the resolution of motion in the *z*-direction is maximized by employing a low scaling factor. Haptic feedback is not the only feedback available to the user; visual feedback is also provided on the computer screens, as shown in Fig. 3. A webcam positioned directly on top of the rotating workpiece and mandrel provides the user with a direct view of the roller-workpiece contact; charts with the roller positions and force help the operator monitor their actions; finally, a graph showing the real-time profile of the workpiece as measured by a laser scanner line completes information on the progress of forming.

## 2.1. Experimental conditions

Having described the haptic spinning set-up, the next sections present two case studies of its potential applications. Some experimental conditions are common to both studies and will be described here.

A wooden mandrel of diameter $D$ = 250 mm, corner radius $r_c$ = 15 mm and straight (90°) wall profile is manufactured and fitted to the machine's tailstock. All figures in Sections 3 and 4 present the wall profile of the mandrel in the $(r, z, \theta = 0)$ plane as shaded in grey. The WRoller coordinates refer to centre of the roller nose, whose radius $r_n$ is 15 mm; to avoid collisions with the mandrel and ensure safety, the mandrel profile is offset by $r_n$ and the obtained line is used as a hard position limit in the manual control of the WRoller. A light grey line represents this limit in the figures.

A blank with diameter $D_0$ = 350 mm is used; this corresponds to a spinning ratio $Z = D_0/D$ of 1.4, a common value in the spinning literature [2].  All experiments are performed on 2 mm-thick blanks of Al-1050-H14. The HDevice is operated by the first author, whose skill derives from two main sources: a 3-day hand spinning workshop with an experienced craftsman, and many spinning trials performed with the CNC machine used in this paper.

## 3. Case study I: force-controlled toolpaths

In CNC spinning, the roller toolpath is usually programmed using a set of positions for the roller to follow. Arai [13] successfully applied a force control approach in shear spinning, and Polyblank and Allwood [14] found a link between mean force and thinning suggesting that force control may be advantageous in conventional spinning, but the approach was never implemented. The ease of use of the HDevice helps applying different force profiles quickly and flexibly so that the resultant toolpath and the outcome on the workpiece deformation can be evaluated.

## 3.1. Design of experiments

The approach is to design three types of target force profiles and to find out the resulting geometry of the WRoller toolpath in position space, as well as the resulting state of the workpiece. The target force profiles are displayed in a chart on one of the screens in front of the operator; the HDevice is used to manually control the WRoller to follow the target profile as closely as possible. The force is measured online and displayed on the same graph so that the operator can monitor their success in matching the target profile.

The portion of the blank undergoing deformation is called the flange. At the start of the process, the flange is at 90° to the mandrel wall; its length $L$ is given by $(D_0 - D)/2$. In the first stage of conventional spinning, the flange is formed to achieve an angle of 45° with the mandrel wall. In this stage, the axial component of the force $F_z$ dominates, while the radial component $F_r$ is negligible. Therefore, we choose to design target force profiles for the axial force $F_z$ as a function of WRoller radial position $W_r$ along the flange until a 45° cone is approximately achieved. Three passes were found to be required to achieve this under the current experimental conditions. We choose to compare three different force profile types: linear, plateauing, and parabolic. For each force profile type, the three passes are designed to have an increasing peak axial force $F_z = 0.8$, 0.9 and 1.0 kN. These values were selected based on empirical data collected in previous position-controlled toolpath trials under the same conditions.

## 3.2. Results

The results of the trials on force-controlled toolpaths are shown in Fig. 4 and 5. The first figure compares the achieved force profiles during manual operation of the WRoller with the target profiles. The plots show the roller axial force $F_z$ as a function of the radial position $W_r$ of the roller; the latter is expressed as quarters of the initial flange length $L$. Looking generally at all profiles, we can see that the achieved force shows larger oscillations in the first quarter of the flange. This can be explained by the larger vibrations experienced by the operator in proximity of the rotating mandrel. Moreover, the operator found it more difficult to follow target force profiles during Pass 3 than during Pass 1 and 2. This is because circumferential variations have been introduced by uneven forming of the flange in the previous passes, making the contact point oscillate axially; and since the workpiece has already been formed considerably in the axial direction, larger distances must be covered by the operator to compensate for gaps between the achieved and target force profile, with consequent delays and oscillations in the commanded axial position and applied force. Comparing the three profile types, we see that for the linear and plateauing force profiles, it was not possible to keep following the increasing force when the WRoller moved beyond three fourths of the flange; in that region, the workpiece simply could not provide enough stiffness. Therefore, the achieved force decreases even if, as shown in Fig. 5, the WRoller moves aggressively in the axial direction. Conversely, the final quarter of the parabolic force profiles was matched with greater accuracy, because the downward curve of the force felt natural to follow.

Fig. 5 shows the toolpass geometries that resulted from following the force profiles shown in Fig. 4. To follow linear and plateauing force profiles and maintain a high force towards the flange edge, the operator had to move
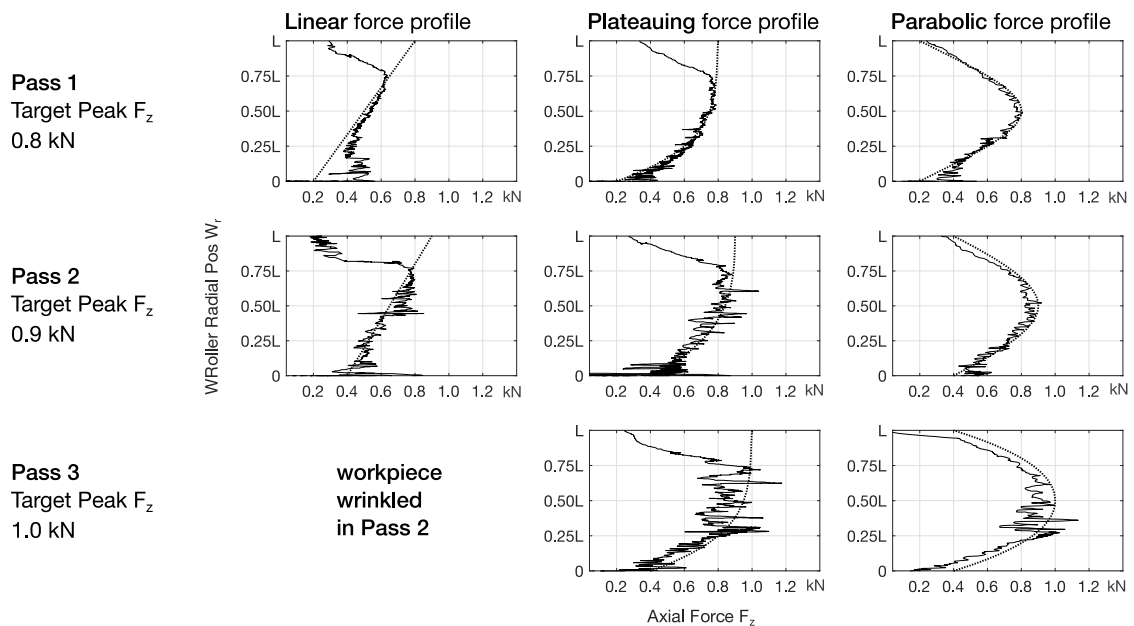


Figure 4. Achieved force profiles (full line) compared to target force profiles (dotted line) for the three types of profiles attempted in the case study on force-controlled toolpaths. The radial position of the WRoller is presented as quarters of the workpiece flange length *L*.
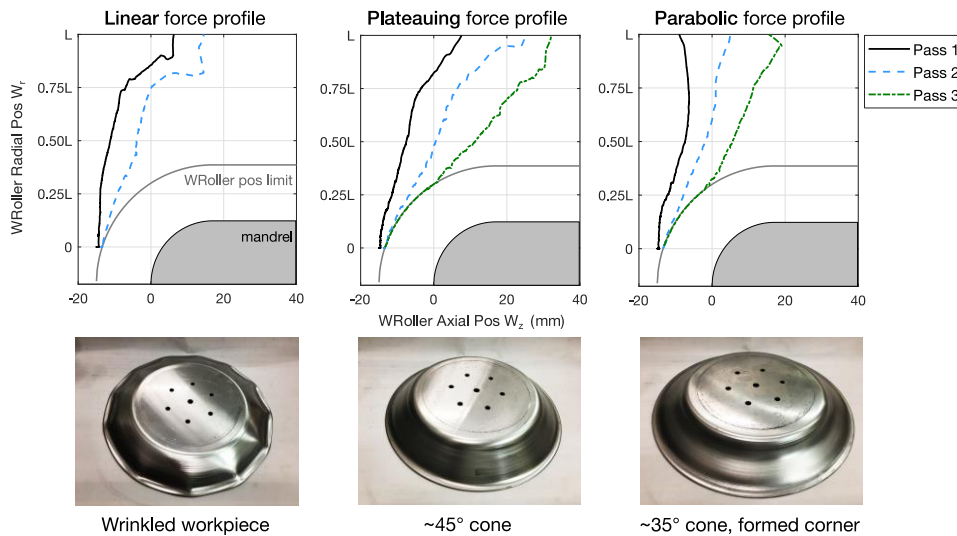
Fig. 5. The toolpasses followed by the human operator in position space while attempting to match the target force profiles of Fig. 4. The resulting workpieces are also shown; the best outcome was achieved by the plateuing-force toolpasses, which formed an approximate 45° cone.

aggressively in the axial direction (the sharp outward radial motion visible towards the end of the linear-force toolpasses is due to the impossibility for the operator to push the workpiece further axially). Therefore, the toolpasses present a convex geometry, with increasing slope at high $W_r$. In the literature, this geometry has been associated to low levels of thinning, but also to a high likelihood of wrinkling [2]. Indeed, during the linear-force Pass 2, the workpiece wrinkled. However, no wrinkling was observed during the plateauing-force toolpasses; this is thought to be because the flange was pushed axially further in the first half of the flange, thus folding back at the edge, and this prevented wrinkling. Parabolic-force toolpasses tend to be concave, especially Pass 1. In these passes, the WRoller position limit was encountered by the operator in the first quarter of the flange, thus making the workpiece adhere to the mandrel. However, the reducing slope of the passes towards the edge of the flange resulted in less deformation in the three passes overall, compared to the plateauing-force toolpasses. Tearing was not observed under these experimental conditions; the max thinning measured in the workpiece after the three passes was 20% for the plateauing and 18% for the parabolic force profiles.

Overall, the plateauing force profiles achieved the best results. However, because the achieved profiles actually decreased towards the edge of the flange, it could be argued that the optimal force profiles are more like parabolic with the peak shifted towards the edge of the flange. How the position and intensity of these peaks should vary throughout the toolpath to avoid wrinkling and minimise thinning is open for investigation.

## 4. Case study II: wrinkling recovery

Wrinkling is a sheet buckling phenomenon originally thought to be caused by excessive circumferential stresses in the flange [2]. Numerical studies carried out more recently have revealed a more complicated picture, with local bending in the roller contact area [15], and have suggested that wrinkling failure is caused by the build-up of residual bending moments [16]. However, a clear connection between toolpath design and wrinkling has not been made yet. Moreover, once wrinkling occurs, the workpiece is generally considered to have failed and is scrapped. Here, we show that it is possible to recover a wrinkled flange to its wrinkle-free state with a single WRoller pass. This finding, if explored further, may lead to clearer rules for toolpath design to avoid and recover wrinkling.

### 4.1. Design of experiments

A wrinkled workpiece was obtained from the previous trials on force control (bottom left of Fig. 5). Then, an attempt was made to flatten the wrinkles in one toolpass by manual control with the HDevice. The operator attempted

to apply teachings received by an experienced spinning craftsman, who usually flattens wrinkles by using an aggressive forward pass while supporting the flange on the other side by use of a wooden stick called 'backstick'. Here, however, no additional support was provided to the flange.

## 4.2. Results

The results of the wrinkling recovery trial are presented in Fig. 6 and 7. The first figure shows the toolpass geometry followed by the operator as well as the force profile recorded; these are compared to two toolpasses from Case Study I: Pass 2 with a linear force profile (which caused the workpiece to wrinkle) and Pass 3 with a plateauing force profile (which achieved the best results). A photograph of the part after wrinkling recovery is also shown. The toolpass succeeded in flattening the wrinkles and brought the flange back to its wrinkle-free state. Its geometry in position space is very similar to the one of plateauing-force Pass 3. However, a striking difference between the two is the large peak in force around the middle of the flange, which occurred as the roller first contacted the wrinkled area (Fig. 7). Moreover, both the wrinkling recovery toolpass and the plateauing-force Pass 3 apply higher force in the first quarter of the flange. This causes the flange to fold back and is believed to create a stress state unfavorable to the formation of wrinkles at the workpiece edge.

Fig. 7 shows the results obtained from measurements of the workpiece shape before, during and after the wrinkles were flattened. The WRoller radial position $W_r$ at which wrinkles are recovered can be extracted from these plots. Wrinkles around the circumference are detected by taking scans of the workpiece every 10° during one rotation and observing the extent of the deviation from the mean workpiece shape. Thus, we see that the initial shape has very large deviation from the mean, while the final shape has very little deviation. By comparing the captured workpiece shapes when the WRoller is just before, at, and just after half of the flange, we notice that the wrinkle amplitude starts
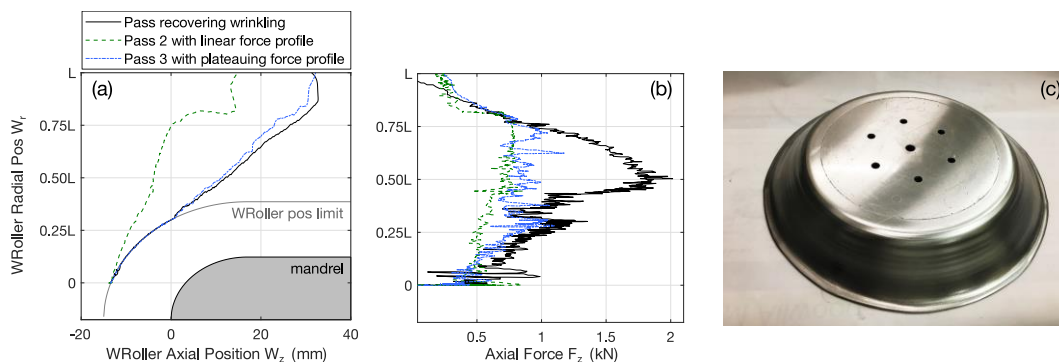


Fig. 6. (a) The toolpass recovering wrinkling, compared to the pass that caused wrinkling and to the pass that achieved best results in the previous force control trials. (b) Force profiles of the toolpasses in (a). (c) Photograph of the recovered, wrinkle-free part.
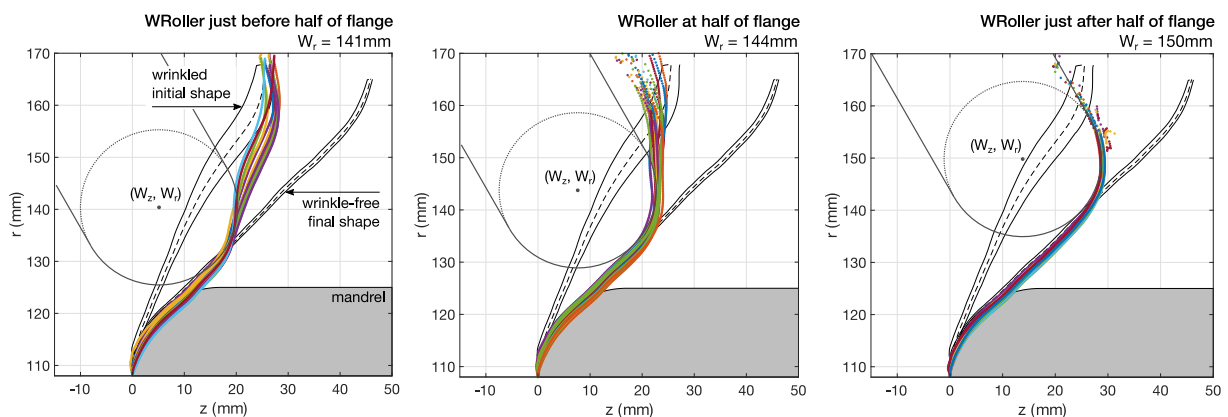


Fig. 7. Evolution of the workpiece shape during the toolpass recovering wrinkling. The initial and final mean workpiece shapes (dashed black lines) are presented with their range of deviation (full black lines); the intermediate shapes are presented as raw laser scans of the workpiece.

decreasing as the flange folds back. As the roller moves past half of the flange ($W_r = 144$ mm), the diameter of the wrinkled section of the workpiece is increased by stretching, and this allows the wrinkles to disappear. However, recovering wrinkling comes at a cost: the max thinning of the part is measured to be 26%, against the 20% found in the 45° cone formed using plateauing-force toolpasses.

## 5. Conclusions and research agenda

The results of the two case studies indicate the great potential for discovery held by haptic metal spinning. Two approaches never reported in the literature were applied quickly and easily notwithstanding the limited experience of the human operator. Given the promising results, a list of further research directions is provided below.

*Force control in conventional spinning.* Force control may provide a new perspective on toolpath design to avoid failure. The way force changes with position along the flange depends on the current shape of the workpiece and on the accumulated work done so far; therefore, designing a force profile to avoid failure may turn out to be more reliable than a positional approach. Future investigations may attempt to design full toolpaths by force control and thus may include design of the radial force $F_r$ in the later stage of the process; hybrid position/force control approaches may also be explored.

*Wrinkling avoidance and recovery.* We have shown that wrinkling is recoverable with an easy-to-design toolpath. Our analysis of the shape evolution data obtained from the sensors is an example of the opportunities offered by haptic metal spinning to reveal relationships between the motion of the roller along the flange, foldback and the likelihood of wrinkling. The operator could feel when wrinkling was about to happen because of the vibrations and the sounds coming from the workpiece. This suggests there may be ways to sense information from the workpiece to correct the toolpath online and avoid wrinkling.

*Capturing craftsmen skills.* Process models of metal spinning are too slow or too imprecise to help designing toolpaths automatically. Instead, spinning craftsmen can react to unexpected variations during a spinning process and avoid failure by performing actions learnt over years of experienced. By having craftsmen use the haptic metal spinning set-up presented, their actions may be studied and parameterised so that widely applicable rules to design full toolpaths may be derived.

## References

[1] C. C. Wong, T. A. Dean, and J. Lin, "A review of spinning, shear forming and flow forming processes," Int. J. Mach. Tools Manuf., vol. 43, no. 14, pp. 1419–1435, 2003.
[2] O. Music, J. M. Allwood, and K. Kawai, "A review of the mechanics of metal spinning," J. Mat. Proc. Tech., vol. 210, no. 1, pp. 3–23, 2010.
[3] M. Hayama, H. Kudo, and T. Shinokura, "Study of the Pass Schedule in Conventional Simple Spinning," Bull. JSME, vol. 13, no. 65, pp. 1358–65, 1970.
[4] J. Liu, H. Yang, and Y. Li, "A study of the stress and strain distributions of first-pass conventional spinning under different roller-traces," J. Mat. Proc. Tech., vol. 129, no. 1, pp. 326–329, 2002.
[5] L. Wang and H. Long, "A study of effects of roller path profiles on tool forces and part wall thickness variation in conventional metal spinning," J. Mat. Proc. Tech., vol. 211, no. 12, pp. 2140–2151, 2011.
[6] J. A. Polyblank, "The Mechanics and Control of Flexible Asymmetric Spinning," University of Cambridge, 2015.
[7] M. K. O'Malley and A. Gupta, "Haptic Interfaces," in HCI beyond the GUI: design for haptic, speech, olfactory and other nontraditional interfaces, P. Kortum, Ed. Morgan Kaufmann, 2008, pp. 25–75.
[8] P. Xia, "Haptics for Product Design and Manufacturing Simulation," IEEE Trans. Haptics, vol. 1412, no. c, pp. 1–1, 2016.
[9] P. F. Hokayem and M. W. Spong, "Bilateral teleoperation: An historical survey," Automatica, vol. 42, no. 12, pp. 2035–2057, 2006.
[10] T. H. Massie and J. K. Salisbury, "The PHANTOM Haptic Interface: A Device for Probing Virtual Objects," Proc. ASME Winter Annu. Meet. Symp. Haptic Interfaces Virtual Environ. Teleoperator Syst. Chicago, IL, Nov. 1994., 1994.
[11] SensAble, "Phantom Desktop User's Guide," 2005. [Online]. Available: http://www.nihonbinary.co.jp/Products/VR/Haptic/Phantom/ PHANTOM Desktop Device Driver Install Guide.pdf. [Accessed: 13-Sep-2018].
[12] O. Music and J. M. Allwood, "Flexible asymmetric spinning," CIRP Ann. - Manuf. Technol., vol. 60, pp. 319–322, 2011.
[13] H. Arai, "Force-controlled metal spinning machine using linear motors," Proc. - IEEE Int. Conf. Robot. Autom., vol. 2006, pp. 4031–36, 2006.
[14] J. A. Polyblank and J. M. Allwood, "Parametric toolpath design in metal spinning," CIRP Ann.-Manuf. Techl., vol. 64, no. 1, pp. 301–4, 2015.
[15] G. Sebastiani, A. Brosius, W. Homberg, and M. Kleiner, "Process Characterization of Sheet Metal Spinning by Means of Finite Elements," Key Eng. Mater., vol. 344, pp. 637–644, 2007.
[16] M. Watson and H. Long, "Wrinkling Failure Mechanics in Metal Spinning," Procedia Eng., vol. 81, pp. 2391–2396, 2014.